Journal of the National Cancer Center 4 (2024) 335–345

Contents lists available at ScienceDirect

Journal of the National Cancer Center

journal homepage: www.elsevier.com/locate/jncc

Full Length Article

Disseminated tumor cells in bone marrow as predictive classifiers for small cell lung cancer patients

Ying Wang[1,†], Jingying Nong[2,†], Baohua Lu[1,†], Yuan Gao[1], Mingming Hu[1], Cen Chen[3], Lina Zhang[4], Jinjing Tan[4], Xiaomei Yang[5,6], Peter Ping Lin[7], Xingsheng Hu[8,*], Tongmei Zhang[1,9,*]

[1] *Department of Medical Oncology, Beijing Chest Hospital, Capital Medical University, Beijing Tuberculosis and Thoracic Tumor Research Institute, Beijing, China*
[2] *Department of Thoracic Surgery, Xuanwu Hospital, Capital Medical University, Beijing, China*
[3] *The First School of Clinical Medicine, Shaanxi University of Chinese Medicine, Xianyang, China*
[4] *Department of Cancer Research Center, Beijing Chest Hospital, Capital Medical University, Beijing Tuberculosis and Thoracic Tumor Research Institute, Beijing, China*
[5] *Beijing Key Laboratory for Tumor Invasion and Metastasis, Department of Biochemistry and Molecular Biology, Capital Medical University, Beijing, China*
[6] *Joint Laboratory for Precision Diagnosis and Treatment Translational Research in Malignant Tumors, Gynecologic Oncology Basic and Clinical Research Laboratory, Capital Medical University, Beijing, China*
[7] *Cytelligen, San Diego, USA*
[8] *Department of Medical Oncology, National Cancer Center/National Clinical Research Center for Cancer/Cancer Hospital, Chinese Academy of Medical Sciences & Peking Union Medical College, Beijing, China*
[9] *Laboratory for Clinical Medicine, Capital Medical University, Beijing, China*

ARTICLE INFO

Keywords:
Bone marrow
Aneuploid DTCs and DTECs
SE-iFISH
Prognosis
SCLC

ABSTRACT

Background: Small cell lung cancer (SCLC) is a highly aggressive disease characterized by early metastasis. Aneuploid CD31$^-$ disseminated tumor cells (DTCs) and CD31$^+$ disseminated tumor endothelial cells (DTECs) residing in the bone marrow are generally considered as the initiators of metastatic process. However, the clinical significance of DTCs and DTECs in SCLC remains poorly understood. The aim of this study is to investigate the clinical implications of diverse subtypes of highly heterogeneous DTCs and DTECs in SCLC patients.

Methods: Subtraction enrichment and immunostaining-fluorescence in situ hybridization (SE-iFISH) was applied to enrich and perform comprehensive morphologic, karyotypic, and phenotypic characterization of aneuploid DTCs and DTECs in 30 patients. Additionally, co-detection of circulating tumor cells (CTCs) and circulating tumor endothelial cells (CTECs) was conducted on 24 of the enrolled patients. Proof-of-concept of the whole exon sequencings (WES) on precisely selected different subtypes of CTCs or DTCs, longitudinally detected from a representative case with pathologically confirmed bone marrow metastasis, was validated to feasibly reveal genetic mutations in these cells.

Results: DTCs, DTECs and their subtypes were readily detectable in SCLC patients. Comparative analysis revealed that the number of DTCs and DTECs was significantly higher than that of their corresponding CTCs and CTECs ($P < 0.001$ for both). Positive detection of disseminated tumor microemboli (DTM) or disseminated tumor endothelial microemboli (DTEM) was associated with inferior survival outcomes ($P = 0.046$ and $P = 0.048$). Patients with EpCAM$^+$ DTCs detectable displayed significantly lower disease control rate (DCR) (16.67% vs 73.33%, $P = 0.019$), reduced median progression-free survival (mPFS) and median overall survival (mOS) compared with those with EpCAM$^-$ DTCs ($P = 0.028$ and $P = 0.002$, respectively). WES analysis indicated that post-treatment DTCs isolated from bone marrow at the time of disease progression shared more homologous somatic gene mutations with pre-treatment CTCs compared with post-treatment CTCs.

Conclusions: Our findings suggest that bone marrow sampling and characterization of DTC subtypes provided a valuable tool for predicting treatment response and the prognosis in SCLC. Moreover, DTCs inherit a greater amount of homologous somatic information from pre-treatment CTCs, indicating their potential role in disease progression and treatment resistance.

* Corresponding authors.
E-mail addresses: huxingsheng66@163.com (X. Hu), tongmeibj@163.com (T. Zhang).
† These authors contributed equally to this work.

https://doi.org/10.1016/j.jncc.2024.07.003
Received 26 March 2024; Received in revised form 27 June 2024; Accepted 20 July 2024

1. Introduction

Small cell lung cancer (SCLC) is the most lethal subtype of lung cancer, characterized by high growth rate and early metastasis.[1] Though the use of immune checkpoint inhibitors (ICIs) has prolonged the overall survival (OS) in SCLC, the majority of patients experience relapse within a short period, and the prognosis remains discouraging.[2] In clinical practice, limited disease SCLC (LD-SCLC) can potentially be cured, with a five-year survival rate of 15–20%,[3] whereas long-term survival is rare in extensive disease SCLC (ED-SCLC).[4,5] Since metastasis is a crucial and lethal step in cancer progression, it is essential to identify tumor cells with aggressive phenotypes to improve treatment response and ultimately achieve better clinical outcomes. SCLC is biologically distinct from other solid tumors due to the presence of early metastases; however, to date, there is few standard techniques to detect occult tumor micrometastases. Though bone marrow aspiration/biopsy is recommended by the National Comprehensive Cancer Network (NCCN) guidelines for SCLC to determine the precise disease stage in selected patients,[6] routine bone marrow smears in clinical practice are insufficient to discriminate tumor cells with distinct aggressive phenotypes. Epithelial-to-mesenchymal transition (EMT) is a cellular differentiation program that is instrumental in tumorigenesis and metastasis.[7] Tumor cells undergoing EMT are more likely to enter the bloodstream and eventually establish metastatic colonies through a reverse process termed mesenchymal-epithelial transition (MET).[8] Epithelial cell adhesion molecule (EpCAM), a marker of the epithelial status of tumor cells, is a multi-functional transmembrane protein involved in the regulation of EMT.[9] By virtue of expressing EpCAM, tumor cells are preferentially involved in the formation of tumor metastasis and are predictive of inferior outcome.[10]

Metastasis formation is commonly initiated by the detachment of cancer cells from primary lesions, leading to their intravasation into the blood stream as circulating tumor cells (CTCs).[11] In addition to $CD31^-$CTCs, which are correlated with tumor relapse and metastasis, $CD31^+$circulating tumor endothelial cells (CTECs) originating from tumor endothelial cells (TECs) within the tumor tissue have also been shown to contribute to tumor growth and disease progression.[12] A fraction of CTCs and CTECs are capable of migrating to distant sites and residing in bone marrow as disseminated tumor cells (DTCs) and disseminated endothelial tumor cells (DTECs).[13] Circulating and disseminated tumor cells found in peripheral blood and bone marrow are commonly considered as metastases-inducing cells capable of predicting poor survival.[14] Furthermore, it is postulated that phenotypic changes occurring within tumor cell subpopulations during the EMT process play a decisive role in regulating their tumorigenic and metastatic functionality.[15,16] Though accumulating evidence supporting EMT as a critical switch controlling tumor cell dissemination and treatment resistance,[17] the functional and clinical significance of the epithelial subtype $EpCAM^+$ DTCs in SCLC remains poorly understood.

In this study, building upon our previous findings regarding EpCAM expression on aneuploid CTCs and CTECs in NSCLC, we employed a novel EpCAM-independent subtraction enrichment (SE) strategy to enrich heterogeneously sized disseminated rare cells (DRCs, i.e., DTCs + DTECs) and circulating rare cells (CRCs, i.e., CTCs + CTECs) in SCLC patients, followed by comprehensive in situ phenotypic, karyotypic, and morphological characterization of DRCs and CRCs performed by the integrated immunostaining fluorescence *in situ* hybridization (iFISH). Recognizing that tumor cells undergoing EMT play a role in chemoresistance and disease progression, we evaluated the potential prognostic value of the epithelial subtype $EpCAM^+$ DTCs and DTECs in predicting therapeutic response and prognosis in SCLC patients receiving first-line treatment.

2. Materials and methods

2.1. Study design

This is a prospective, non-interventional, multicentre study (see study design and workflow diagram in Fig. 1) which was conducted at three teaching medical centers (Beijing Chest Hospital, Capital Medical University; Cancer Hospital, Chinese Academy of Medical Sciences and Peking Union Medical College; and Beijing Xuanwu Hospital, Capital Medical University). Briefly, pathologically confirmed unresectable

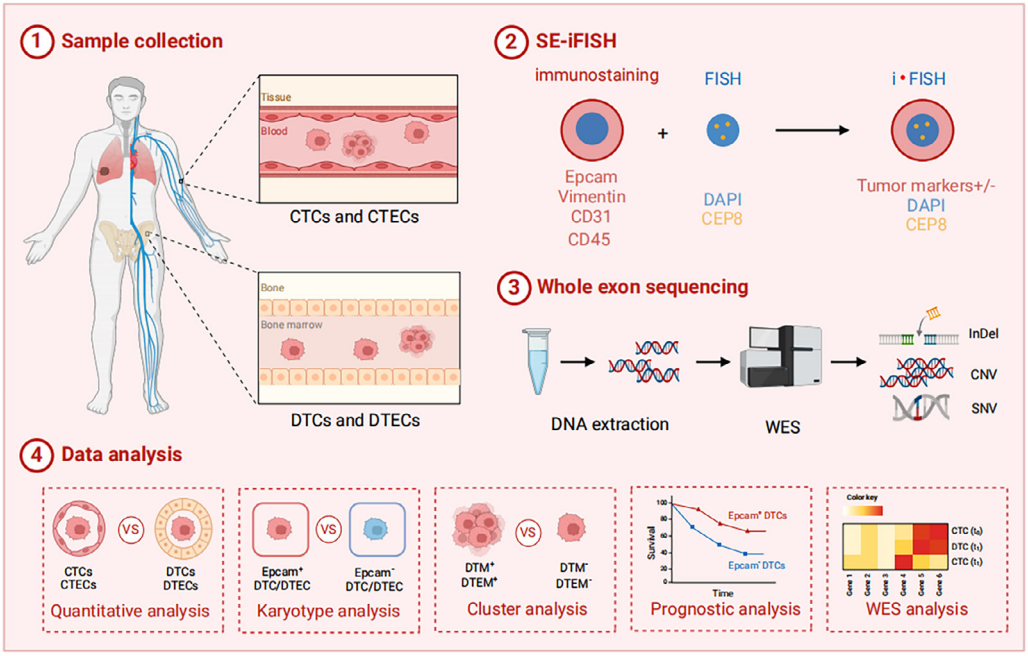

Fig. 1. The overall design of this study. Created with BioRender.com. CEP8, centromere probe 8; CNV, copy number variation; CTCs, circulating tumor cells; CTECs, circulating tumor endothelial cells; DAPI, 4,6-diamino-2-phenyl indole; DNA, deoxyribo nucleic acid; DTCs, disseminated tumor cells; DTECs, disseminated tumor endothelial cells; DTEM, disseminated tumor endothelial microemboli; DTM, disseminated tumor microemboli; Epcam, Epithelial cell adhesion molecule; InDel, insertion deletion; SE-iFISH, subtraction enrichment and immunostaining-fluorescence in situ hybridization; SNV, single nucleotide variation; WES, whole exon sequencing.

SCLC patients aged 18–75 years and had a performance status (PS) ≤2, with adequate organ function and evaluable tumor lesions were eligible for this study. Patients with a history of other malignant tumors were excluded. All patients received the standard first-line treatment according to NCCN/Chinese Society of Clinical Oncology (CSCO) guidelines were ultimately eligible for final analysis. The disease stage was categorized by imaging evaluation including brain magnetic resonance imaging (MRI), computed tomography (CT) of the chest and abdomen, radionuclide bone scanning, or positron emission tomography (PET) scanning. Six to seven weeks (two cycles) after treatment initiation, evaluation of clinical response was performed by means of CT or MRI according to Response Evaluation Criteria in Solid Tumors (RECIST) version 1.1 criteria. Responses were recorded as partial response (PR), progressive disease (PD), or stable disease (SD). Bone marrow and their paired blood samples were collected from pre-treatment SCLC patients. Quantitative comparison of DRCs and CRCs was conducted and the relationship between $EpCAM^+$ DTCs and treatment response was evaluated. Univariate survival analysis was applied to evaluate the prognostic significance of $EpCAM^+$ DTCs and $EpCAM^+$ DTECs in SCLC patients. This study is being conducted in accordance with the Declaration of Helsinki Principles. All patients gave written informed consent.

2.2. SE-iFISH

SE-iFISH was performed according to the manufacturers' instructions (Cytelligen, San Diego, CA, USA). Briefly, bone marrow and peripheral blood samples were collected from each patient before treatment administration. Samples were washed with PBS and subsequently loaded on the nonhematopoietic cell separation matrix, followed by centrifugation at 450 g for 5 min at room temperature to remove sedimented RBCs. Supernatants containing WBCs and tumor cells were incubated with anti-CD45 monoclonal antibody-coated magnetic beads (Promega, Madison, WI). WBC-bound immuno-beads were depleted by means of a magnetic separator suitable for 50 ml tubes (Cytelligen). The remaining WBC-free supernatants containing tumor cells were centrifuged and resuspended in PBS, followed by spreading onto a Cytelligen-formatted slide and dried overnight for subsequent iFISH processing.

With regard to iFISH, the coated slides containing dried monolayer cells were rinsed with PBS, followed by dehydration and subsequent FISH hybridization with the centromere probe 8 (CEP8 SpectrumOrange, Vysis, Abbott Laboratories, Chicago, IL, USA) for 3 h utilizing a ThermoBrite FISH Slides Processing System (Leica Biosystems, Buffalo Grove, IL, USA). Samples were subsequently incubated with the indicated monoclonal antibodies against cellular proteins, including Alexa Fluor (AF)594-anti-CD45 (Clone 9.4), Cy5-anti-CD31 (Clone WM59), AF488-anti-EpCAM (Clone 9C4), and Cy7-anti-vimentin (Vim) (Clone 1D3) for 20 min in the dark. After washing, the mounting media containing DAPI (Vector Laboratories, Burlingame, CA, USA) was added to the samples. Conjugation of all the different fluorescent dyes to the applied antibodies was performed at Cytelligen.

CTC slides were automatically scanned and analyzed by the Metafer-i•FISH imaging system. Depicted in supplementary Table 1, the identification criteria for aneuploid CTCs and DTCs includes the following: $DAPI^+/CD45^-/CD31^-/EpCAM^{+or-}/Vim^{+or-}$ aneuploid cells. Criteria for aneuploid CTECs and DTECs includes: $DAPI^+/CD45^-/CD31^+/EpCAM^{+or-}/Vim^{+or-}$ aneuploid cells. Small cell: ≤5 μm; large cell: >5 μm. A cell cluster is defined as more than two individual cells with clear nuclei adjacently staying together. Comprehensive characterization and subcategorization of aneuploid tumor cells were performed upon cell size, tumor marker expression and the degree of aneuploidy.

2.3. Whole exon sequencing (WES) and data processing

WES was additionally performed on samples that are periodically collected from one patient who was pathologically confirmed bone marrow metastasis at the time of disease progression. Samples from the subject covered pre-treatment CTCs, post-treatment CTCs and DTCs at the date of disease progression. Non-laser microscopic single-cell manipulator (n-MSM, Cytelligen)[18] was used to specifically isolate three of single CTCs or DTCs in each sample. The whole-genome amplification and sequencing library was prepared using the SMARTer® PicoPLEX® Gold Single-Cell DNA-Seq kit (Takara Biosystems) REPLI-g Single Cell Kit (Qiagen, Germany) following the manufacturer's operation manual. The library was quality checked and sequenced on an Illumina HiSeq X Ten platform and the sequencing depth is 100×. Reads sequenced from each sample were first processed via fastp (v0.20.0) to cut adaptor sequences and trim based with low quality. Then, clean reads were mapped to b37 human genome via BWA-0.7.17. Sites harboring single nucleotide variation (SNV) and insertion deletion (InDel) were called employing GATK (v4.1.2) with the pipeline of Mutect2. On the other hand, copy number variation (CNV) regions were called via Control-FREEC v11.5. To extract genes affected by CNV regions, intersect in bed tools v2.28.0 toolset was used to identify intersection between CNV regions and human gene models recorded in Ensembl release 75.

Variant allele frequency was calculated for each filtered SNV and InDel site. Then, hierarchical clustering was conducted for all samples based on variant allele frequencies of filtered sites, number of mutations on genes and copy numbers of genes, respectively. Following that, K-means clustering was conducted for all samples based on the same data mentioned above. Somatic signatures were identified for each sample via the R package. To determine how many signatures should be identified for each sample, the residuals sum of squares and the explained variance between the observed and fitted mutational spectrum were calculated for a series of numbers of signatures. All samples were clustered based on distributions of motifs in corresponding mutational spectrums. Clonal structures were analyzed via PyClone v0.13.1 for different sample groups based on reference and alternative allele counts of shared mutations and copy number of regions covering these mutations. Density, parallel coordinates, and scatter drawings were plotted to show clonal structure changing among different samples in the same group.

2.4. Statistical analysis

All statistical analyses were conducted using SPSS 25.0 software (Chicago, IL, USA) and GraphPad Prism 8.0 (GraphPad Software Inc., San Diego, CA). Chi-square test and Fisher's exact test were used to compare categorical data. Continuous variables were described as the mean ± standard deviation or the median and interquartile range (IQR) where appropriate and compared using the Mann–Whitney test. The primary endpoint was OS and secondary endpoints included progression-free survival (PFS) and disease control rate (DCR). Kaplan–Meier survival plots were generated based on DTCs and DTECs subtypes and compared using log-rank tests. All P values were two-sided. $P < 0.05$ was considered statistically significant.

3. Results

3.1. Patients' characteristics and co-detection of DTCs and DTECs in SCLC

A total of 30 eligible SCLC patients, including 15 limited stage and 15 extensive stage subjects, were prospectively enrolled from February 2018 to January 2020. The clinical characteristics of the included patients are listed in Table 1. Six-channel iFISH was applied to perform a comprehensively phenotypic and karyotypic characterization of diverse subtypes of aneuploid DTCs and DTECs. Representative images of aneuploid DTCs or DTECs identified by iFISH are displayed in Fig. 2. As exhibited in Fig. 2A–C, DTCs show different degrees of aneuploidy, heterogeneous morphologies, and phenotypes including large multiploid (≥ pentasomy 8) $EpCAM^+/Vim^-/CD31^-$ DTCs ($_LCTC^{multi}$, Fig. 2A), small $EpCAM^-/Vim^+/CD31^-$ triploid DTCs ($_SDTC^{tri}$, Fig. 2B), and a triploid $EpCAM^-/Vim^-/CD31^-$ DTCs (Fig. 2C). Additionally, a large multiploid

Table 1
Clinical features of enrolled SCLC patients.

Characteristics	Limited stage patients, n (%)	Extensive stage patients, n (%)
Age, years		
≥60	11 (73.33)	10 (66.67)
<60	4 (26.67)	5 (33.33)
Sex		
Male	12 (80.00)	12 (80.00)
Female	3 (20.00)	3 (20.00)
Smoking history		
Yes	13 (86.67)	12 (80.00)
No	2 (13.33)	3 (20.00)
PS		
0-1	14 (100.00)	13 (86.67)
2	1 (0)	2 (13.33)
Liver metastasis		
Yes	0 (0)	3 (20.00)
No	15 (100.00)	12 (80.00)
Bone metastasis		
Yes	0 (0)	4 (26.67)
No	15 (100.00)	11 (73.33)
Brain metastasis		
Yes	0 (0)	2 (13.33)
No	15 (100.00)	13 (86.67)
Treatment response		
PR	11 (73.33)	12 (80.00)
SD	2 (13.33)	2 (13.33)
PD	2 (13.33)	1 (6.67)
Treatment regimens		
CE + radiotherapy	11 (73.33)	2 (13.33)
EP + radiotherapy	2 (13.33)	0 (0)
CE	1 (6.67)	10 (66.67)
EP	1 (6.67)	1 (6.67)
CE+ ICI	0 (0)	2 (13.33)

Abbreviations: CE, carboplatin and etoposide; EP, etoposide and cisplatin; ICI, Immune checkpoint inhibitors; PD, progressive disease; PR, partial response; PS, performance status; SD, stable disease; VALSG, Veterans Administration Lung Study Group.

DTEC ($_{L}DTEC^{multi}$) with phenotypes of $EpCAM^{+}/Vim^{-}/CD31^{+}$ is displayed in Fig. 2D. A small triploid $EpCAM^{-}/Vim^{-}/CD31^{+}$ DTEC is exhibited in Fig. 2E. Fig. 2F reveals an $EpCAM^{+}/Vim^{-}/CD31^{+}$ fusogenic disseminated tumor microemboli (DTM) consisting of two cells.

3.2. Quantification analysis of DTCs and DTECs

Quantification of DTCs and DTECs was performed and results revealed DTCs presence in 28 out of 30 (93.33%) patients and $EpCAM^{+}$ DTCs could be detected in 8 out of 30 patients (26.67%). As for DTECs, the positivity rate is 83.33% (25/30) and $EpCAM^{+}$ DTECs were identified in 19 out of 30 patients (63.33%).

Among the 30 enrolled subjects, 24 were available for the paired CTCs and CTECs detection. Obtained data demonstrated CTCs were identified in 22 out of 24 (91.67%) subjects and $EpCAM^{+}$ CTCs could be detected in 7 out of 24 patients (29.17%). However, the positive detection of $EpCAM^{+}$ CTCs was not consistent with that of $EpCAM^{+}$ DTCs and only one patient harbored both EpCAM phenotype CTCs and DTCs. With regard to CTECs, result revealed the presence of CTECs in 15 out of 24 (62.50%) patients, while $EpCAM^{+}$ CTECs were detected in 41.67% (10/24) patients and half of them meanwhile harbored $EpCAM^{+}$ DTECs.

As for quantitative distribution, the number of DTCs and DTECs in the enrolled patients ranged from 0 to 1380/3 ml and 0 to 75/3 ml while the CTCs and CTECs counts in the subjects ranged from 0 to 277/3 ml and 0 to 5/3 ml respectively (Fig. 3Aa-b). Comparative analysis was performed between DTCs and CTCs, as revealed in Fig. 3Ba, before treatment the median values were 61.5 (red, IQR 13-245) for DTCs and 1 (blue, IQR 0.5-2) for CTCs, the number of DTCs was significantly higher than that of CTCs ($P < 0.001$). We further conducted quantity comparation of DTECs and CTECs, shown in Fig. 3B, the median numbers of DTECs and CTECs were 20.5 (red, IQR 2-101) and 0.50 (blue, IQR 0-1) respectively, significant quantitative difference was observed between the two groups ($P < 0.001$).

Quantification of heterogeneously phenotypes of aneuploid DTCs and DTECs in 30 samples is depicted in Fig. 3C and the compositional waterfall map in Fig. 3D. As revealed in Fig. 3C, among a total of 5954 DTCs enriched from the totality of bone marrow samples, there were 745 EpCAM positive cells (745/5954=12.51%, blue in Fig. 3D-a) and 5209 EpCAM negative cells (5209/5954=87.49%, green in Fig. 3D-a). Trisomy 8 constituted the principal karyotype for $EpCAM^{+}$ DTCs (360 cells, 360/5054=6.05%, blue), followed by tetrasomy (292 cells, 292/5954=4.90%, blue), monosomy (71 cells, 71/5954=1.19%, blue) and pentasomy 8 (22 cells, 22/5954=0.37%, blue), whereas $EpCAM^{-}$ DTCs were heterogeneous in varieties of aneuploidy degrees of chr8 from trisomy (2890 cells, 2890/5954=48.54%, green), tetrasomy (1303 cells, 1303/5954=21.88%, green), pentasomy (770 cells, 770/5954=12.93%, green) to monosomy 8 (246 cells, 246/5954=4.13%,green). Significant karyotype difference was observed between $EpCAM^{+}$ DTCs and $EpCAM^{-}$ DTCs ($P < 0.001$).

Further numerical analysis of aneuploid DTECs and their EpCAM positive subtypes was performed and result indicated pentasomy 8 consisted the majority of both $EpCAM^{+}$ DTECs and $EpCAM^{-}$ DTCs. Among those $EpCAM^{+}$ DTECs, no haploid and triploid cells were detected and the ratios of tetraploid and multiploid cells were 0.02% and 50.97%. As for $EpCAM^{-}$ DTECs, there are no haploid and tetraploid cells identified and the positivity of triploid and multiploid cells were 0.71% and 48.29% respectively.

3.3. Prognostic roles of DTM and DTEM in SCLC patients

The above analysis illustrates the counts of DTCs and DTECs are significantly higher than their corresponding CTCs and CTECs. These abundant tumor cells residing in bone marrow are heterogeneous and com-

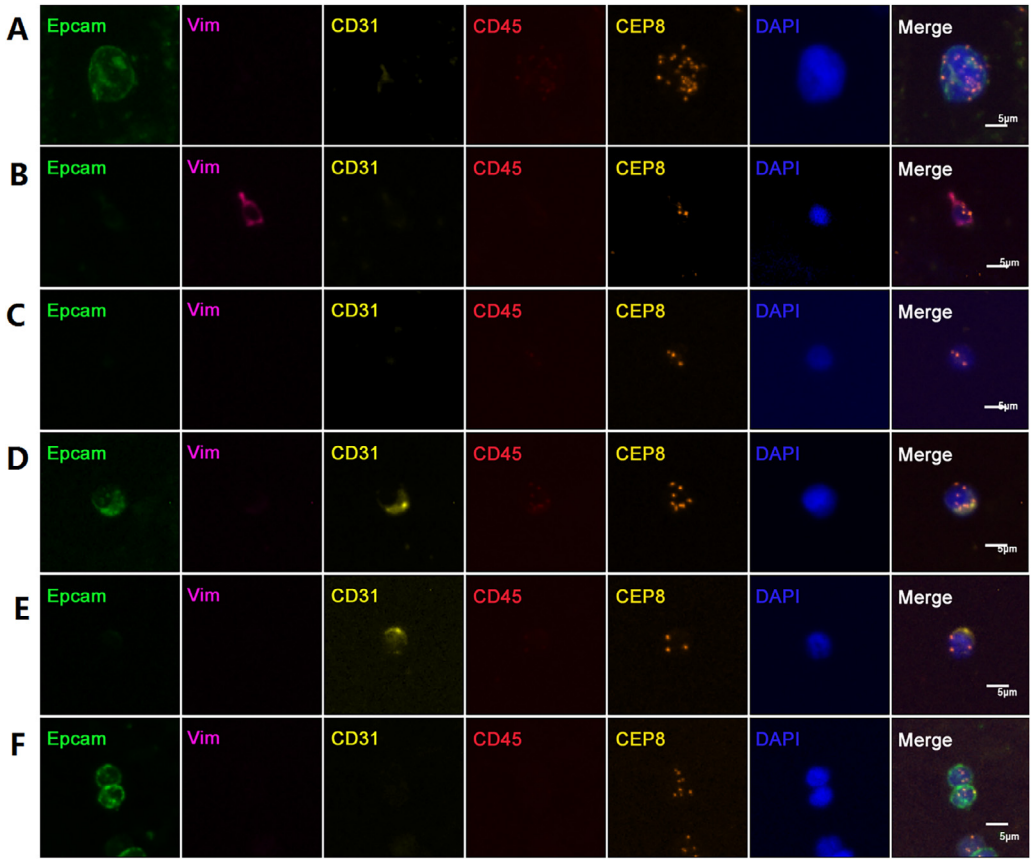

Fig. 2. Representative images of heterogeneous aneuploid DTCs and DTECs expressing EpCAM or Vim in SCLC patients by SE-iFISH. (A) A representative image of a large multiploid (≥ pentasomy 8) EpCAM$^+$/Vim$^-$/CD31$^-$ DTCs ($_L$DTC^{multi}). (B) A representative image of a small EpCAM$^-$/Vim$^+$/CD31$^-$ triploid DTCs ($_S$DTC^{tri}). (C) A representative image of a small EpCAM$^-$/Vim$^-$/CD31$^-$ triploid DTCs. (D) A representative image of a large multiploid DTECs with phenotypes of EpCAM$^+$/Vim$^-$/CD31$^+$ ($_L$DTEC^{multi}). (E) A representative image of a small triploid EpCAM$^-$/Vim$^-$/CD31$^+$ DTEC. (F) A representative image of an EpCAM$^+$/Vim$^-$/CD31$^-$ fusogenic disseminated tumor microemboli. CEP8, centromere probe 8; DAPI, 4,6-diamino-2-phenyl indole. DTCs, disseminated tumor cells; DTECs, disseminated tumor endothelial cells; DTEM, disseminated tumor endothelial microemboli; DTM, disseminated tumor microemboli; Epcam, epithelial cell adhesion molecule; SCLC, small cell lung cancer; SE-iFISH, subtraction enrichment and immunostaining-fluorescence in situ hybridization; Vim, vimentin.

monly exist as single cells, but can also assemble to form clusters. In our study, the DTC and DTEC clusters, also termed as disseminated tumor microemboli (DTM) and disseminated tumor endothelial microemboli (DTEM), were progressively investigated. Obtained data indicated that the DTM were identified in 8 out of 30 patients (26.67%). While the positive rate of DTEM is 46.67% (14/30), their contemporaneous circulating tumor microemboli (CTM) and circulating tumor endothelial microemboli (CTEM) were detected in only 8.33% (2/24) and 12.50% (3/24) patients respectively.

The prognostic significance of DTM and DTEM was investigated and their relationship with survival was analyzed utilizing Kaplan-Meier plots. Patients with the presence of DTM demonstrated a significantly shorter mOS of 11.53 months (95% CI: 9.98–13.08 months) compared with a mOS of 23.53 months (95% CI: 15.42–31.64 months) for those with the absence of DTM ($P = 0.046$, log-rank test, Fig. 4A). Similar results were observed with respect to the relationship between DTEM and OS. Patients with DTEM had significantly reduced mOS compared with those without DTEM [11.80 (95% CI: 10.28–13.32) months vs. 20.60 (95% CI: 10.08–31.13) months, $P = 0.048$, log-rank test, Fig. 4B].

3.4. WES of CTCs and DTCs from a typical case with bone marrow metastasis

Since bone marrow has been primarily envisioned as the home organ of CTCs and bone marrow niche can provide microenvironment for supporting tumor cell dormancy,[19] we further investigated the molecular heterogeneity of CTCs and DTCs at different time points. WES was performed in three samples covering CTCs before treatment administration (t_0) and CTCs and DTCs at the date of disease progression (t_1) from an ED-SCLC patient who was pathologically confirmed bone marrow metastasis at the time of tumor progression. Systemic comparison was conducted between CTCs(t_0), CTCs(t_1), and DTCs(t_1). Shown in Fig. 5A, our results demonstrated that gene mutation number in CTCs(t_1) and DTCs(t_1) is much lower than that of CTCs(t_0). Moreover, compared with CTCs(t_1), DTCs(t_1) in bone marrow share more homologous somatic gene mutations with CTCs(t_0). The number of SNV genotypes in each sample was analyzed and depicted in Fig. 5B. Results confirmed 30 and 36 SNV mutations in CTCs(t_0) and CTCs(t_1), respectively. The overlapping area indicated that there were 11 identical SNV mutations shared between the two samples. Similar analysis was conducted between CTCs(t_0) and DTCs(t_1). Obtained data revealed the number of SNV mutations was 24 in DTCs(t_1), with 16 overlapping mutations. Pan-cancer mutated genes were listed in Fig. 5C. There were 4 gene mutations identified in all three samples, 7 mutations were specific to CTC(t_0), 1 mutation was specific to DTC(t_1), and 12 mutations were specific to CTC(t_1), indicating intra-tumor genomic heterogeneity both spatially and temporally.

3.5. EpCAM$^+$ DTCs correlated with treatment response and predicted poor PFS and OS

To reveal the role of epithelial-type tumor cells in treatment response assessment, analysis was conducted to investigate whether the existence of particular subtypes of EpCAM$^+$ DTCs or EpCAM$^+$ DTECs correlated

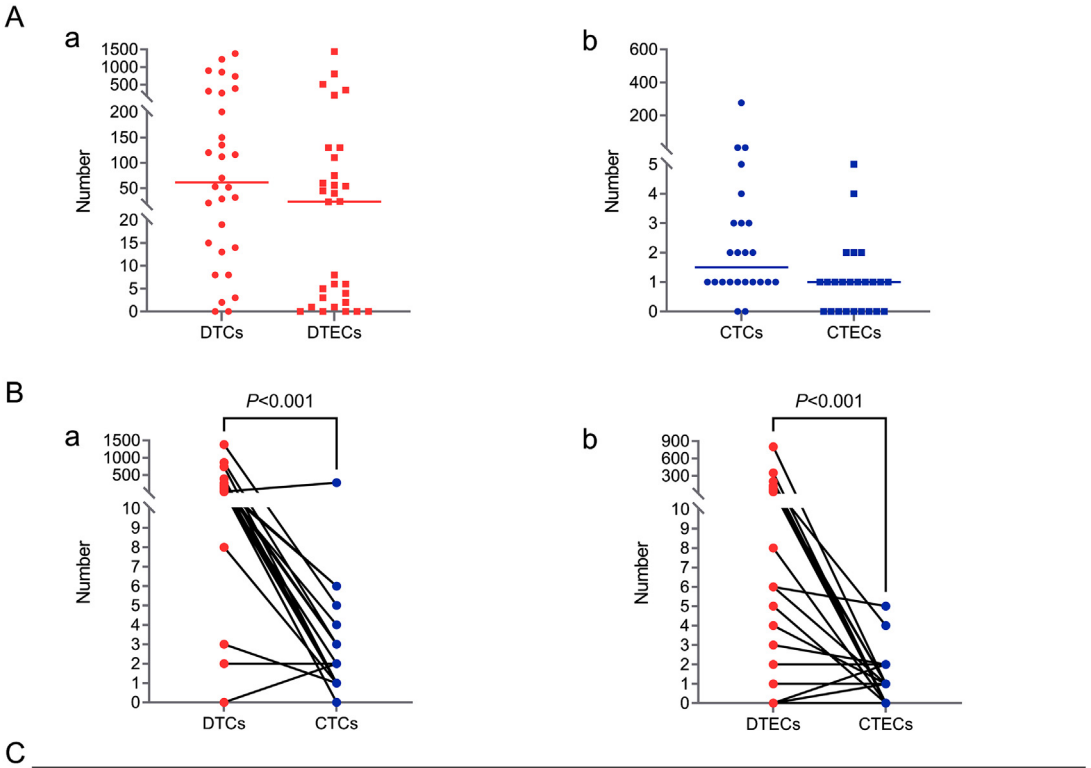

C

	Total		EpCAM postive		EpCAM negitive	
			Numbers	Percentage, % (Number/Total)	Numbers	Percentage, % (Number/Total)
DTC	5954	Multiploid	22	0.37	770	12.93
		Tetraploid	292	4.90	1303	21.88
		Triploid	360	6.05	2890	48.54
		Monoploid	71	1.19	246	4.13
		Sum	745	12.51	5209	87.49
DTEC	4063	Multiploid	2071	50.97	1962	48.29
		Tetraploid	1	0.02	0	0.00
		Triploid	0	0.00	29	0.71
		Monoploid	0	0.00	0	0.00
		Sum	2072	51.00	1991	49.00

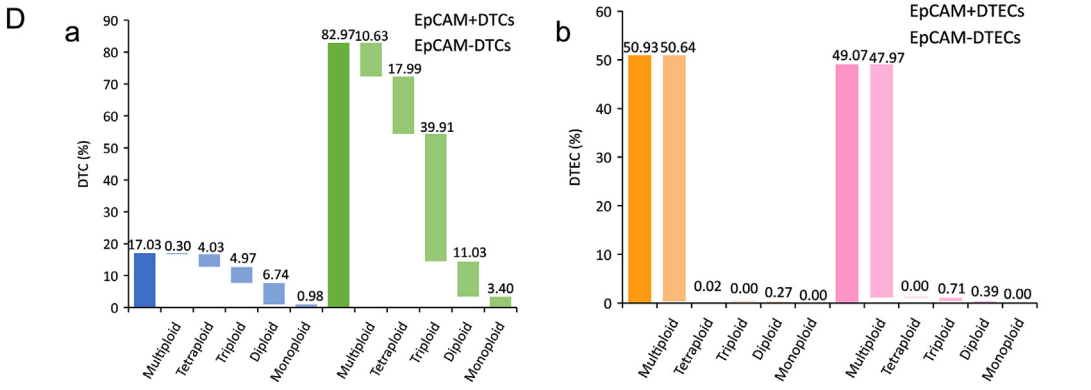

Fig. 3. Quantification and molecular characterization of co-detected diverse subtypes of aneuploid disseminated rare cells (DTCs + DTECs) and circulating rare cells (CTCs + CTECs). (A-a) Quantitive distribution of pre-treatment DTCs and DTECs. (A-b) Quantitive distribution of pre-treatment CTCs and CTECs. (B-a) Shown are numbers comparison of detected DTCs and CTCs in each patient. Paired DTC and CTC values are connected by solid lines ($P < 0.001$, Wilcoxon signed-rank test). (B-b) Shown are numbers comparison of detected DTECs and CTECs in each patient. Paired DTEC and CTEC values are connected by solid lines ($P < 0.001$, Wilcoxon signed-rank test). (C) Quantitative analysis of molecularly characterized DTCs and DTECs with different phenotypes. Highest proportions of different subtypes are highlighted in red font. (D) Compositions of DTC (D-a) and DTEC (D-b) subtypes are depicted in a waterfall map. CTCs, circulating tumor cells; CTECs, circulating tumor endothelial cells; DTCs, disseminated tumor cells; DTECs, disseminated tumor endothelial cells.

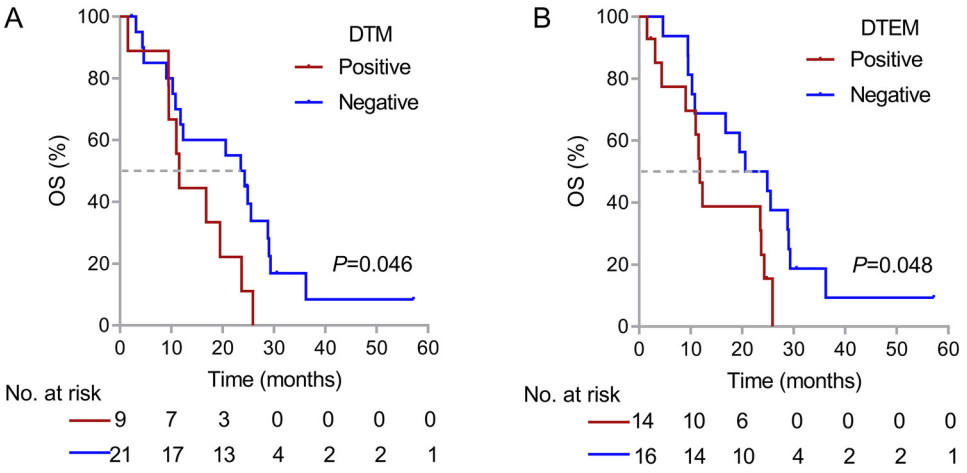

Fig. 4. Kaplan–Meier survival analysis of DTM and DTEM on SCLC patients' OS. (A) The OS curves of SCLC patients with negative and positive DTM. (B) The OS curves of SCLC patients with negative and positive DTEM. DTM, disseminated tumor microemboli; DTEM, disseminated tumor endothelial microemboli; OS, overall survival; SCLC, small cell lung cancer.

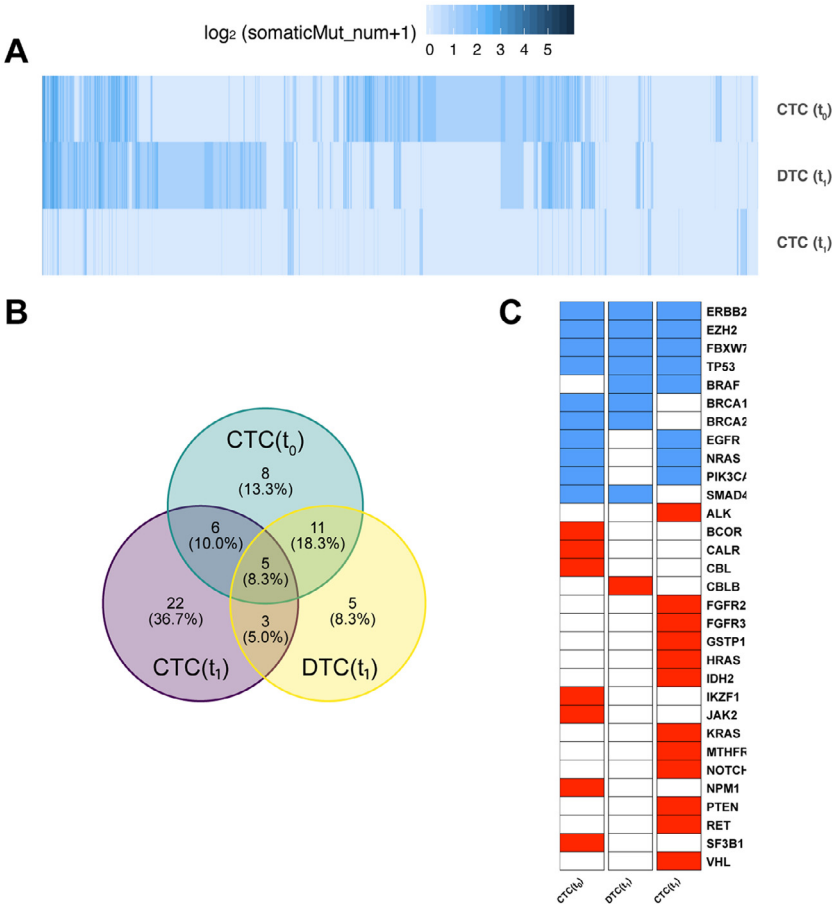

Fig. 5. WES of CTCs and DTCs from an extensive disease small cell lung cancer patient with pathologically confirmed bone marrow metastasis at the time of tumor progression. (A) Gene mutation distribution of the three samples is graphically depicted by the log value and summarized in the heatmap. (B) Venn diagram showed distribution of the overlap SNV mutations between each sample. (C) Pan-cancer mutation genes are listed as overlapped mutation genes (blue) and sample specific mutated genes (red). CTCs, circulating tumor cells; DTCs, disseminated tumor cells; WES, whole exon sequencing.

with patients' response to initial treatment regimens. All enrolled patients received standard treatment for at least 2 cycles and were available to therapeutic efficiency evaluation, 23 (76.67%) achieved PR, 4 (13.33%) showed SD, and 3 (10.00%) developed PD rapidly (Fig. 6A). Obtained results indicated that the positive detection of EpCAM$^+$ DTCs were significantly correlated with a decreased DCR ($P = 0.019$ Fig. 6B). However, no statistical significance in DCR was achieved between EpCAM$^+$ DTECs and EpCAM$^-$ DTECs cohort patients ($P = 0.449$, Fig. 6B).

In light of the truth that tumor cells with the positive expression of EpCAM may be indicative biomarkers for dismal prognosis, univariate analysis was performed to investigate the association between EpCAM$^+$ DTCs and PFS or OS. Detailed progressive clinical status of each patient throughout therapy is shown in Fig. 7A. Patients harboring EpCAM$^+$ DTCs had a mPFS of 8.97 months (95% CI: 2.10–15.84 months), which was significantly shorter than 10.63 months (95% CI: 8.53–12.74 months) for patients possessing EpCAM$^-$ DTCs ($P = 0.028$, log-rank test, Fig. 7Ba). Similarly, patients have EpCAM$^+$DTCs had a significantly decreased mOS of 11.00 months (95% CI: 8.15–13.86 months) than 24.30 months (95% CI: 18.14–30.46 months) for patients with EpCAM$^-$ DTCs ($P = 0.002$, log-rank test, Fig. 7Bd). Additional analysis of subgroup patients classified upon disease stages was conducted. Results revealed that compared to patients with EpCAM$^-$

A

Treatment response	EpCAM⁺ DTCs		Total
	Positive	Negative	
PR	5	18	23
SD	0	4	4
PD	3	0	3

Treatment response	EpCAM⁺ DTECs		Total
	Positive	Negative	
PR	13	10	23
SD	3	1	4
PD	3	0	3

B

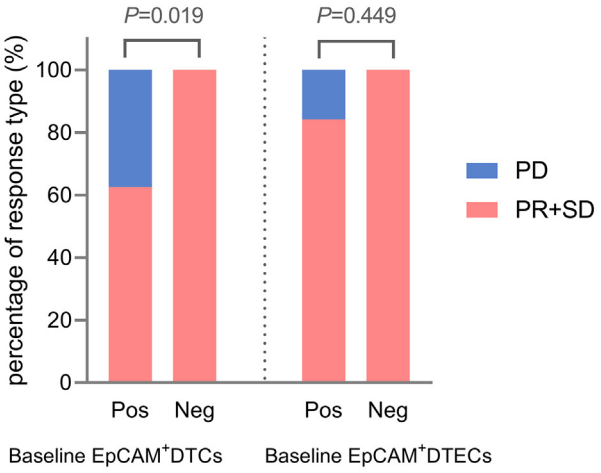

Fig. 6. The relationship between EpCAM⁺ DTCs, EpCAM⁺ DTECs, and DCR in SCLC. (A) Response after two cycles of treatment administration in all enrolled SCLC patients. (B) Patients with positive detection of EpCAM⁺ DTCs were significantly correlated with a decreased DCR ($P = 0.019$), but no statistical difference in DCR was observed between EpCAM⁺ DTECs and EpCAM⁻ DTECs cohort patients ($P = 0.449$). DCR, disease control rate; DTC, disseminated tumor cells; DTEC, disseminated tumor endothelial cells; Neg, negative; PD, progressive disease; Pos, positive; PR, partial response; SD, stable disease; SCLC, small cell lung cancer.

DTCs, patients with EpCAM⁺ DTCs showed significantly shorter PFS [13.73(95% CI:2.22–25.24) months vs. 3.6(95% CI: 0.27–6.99) months, $P < 0.001$, log-rank test, Fig. 7Bb] and OS [25.53(95% CI: 23.95–27.12) months vs. 4.37(95% CI: 0.00–8.92) months, $P = 0.001$, log-rank test, Fig. 7Be] in LD-SCLC patients. However, no statistical significance was achieved between the two groups in PFS [9.47(95% CI: 9.17–9.77) months vs. 6.13(95% CI: 2.16–10.10) months, $P = 0.569$, log-rank test, Fig. 7Bc] or OS [11.53(95% CI: 10.39–12.67) months vs. 16.80(95% CI: 0.00–35.88) months, $P = 0.563$, log-rank test, Fig. 7Bf] in ED-SCLC patients.

Correlation of EpCAM⁺ DTECs with prognosis was as well analyzed utilizing Kaplan-Meier plots. Depicted in supplementary Fig. 1A, baseline EpCAM⁺ DTECs did not demonstrate significant correlation with patients' poorer PFS [9.33(95% CI: 8.59–10.07) months vs. 10.63(95% CI: 8.69–12.57) months, $P = 0.464$, log-rank test]. Shown in supplementary Fig. 1B, though patients in EpCAM⁺ DTECs cohort showed a shorter mOS than those in EpCAM⁻ DTECs cohorts, there is no statistical significance between the two cohorts (12.30 m vs 24.87 m, $P = 0.080$, Log rank test).

4. Discussion

This prospective, non-interventional study represents a pioneering effort to offer clinical and genetic evidence regarding the diverse subpopulations of heterogenous DTCs and DTECs in bone marrow. The study also places particular emphasis on evaluating the clinical significance of the specific epithelial subtype EpCAM⁺ DTCs in SCLC patients.

The limited number of surgically resectable patients[20,21] poses a major challenge in SCLC research, as obtaining tissue samples from these patients is not always feasible in clinical practice. Although the detection and analysis of CTCs from blood samples provides a non-invasive alternative for assessing tumor cell heterogeneity and advancing our understanding of tumor biology,[22] the survival of CTCs is hindered by various factors such as anoikis, shear forces, and immune system elimination.[23] The rarity of CTCs presents significant challenges, and exploring alternative sampling locations is urgently needed to fully unlock the prognostic and predictive potential of CTCs for optimizing the clinical management of SCLC patients.[24] Bone marrow represents an accessible and nurturing nest for CTCs, as the fenestrated endothelium of capillary beds facilitates tumor cell extravasation.[25] Once they exist the bloodstream, CTCs reside in the bone marrow as DTCs and utilize perivascular niche to survive and colonize.[26] Previous studies have demonstrated that bone marrow can serve as a reliable reservoir, and the persistence of DTCs is commonly related to metastasis and disease progression.[27] However, a bone marrow aspiration is not recommended according to current NCCN guidelines for SCLC.[6] In this study, DTCs and DTECs residing in bone marrow and contemporaneous CTCs and CTECs in blood are detected and comprehensively characterized. Comparative analysis revealed that DTCs and DTECs were significantly more abundant than their corresponding CTCs and CTECs in blood. These findings are consistent with previous investigation in breast cancer patients,[15] implying that the bone marrow provides a unique advantage in terms of tumor cell quantity and may serve as a more optimal alternative sample location for studying SCLC. Furthermore, WES analysis revealed spatial and tem-

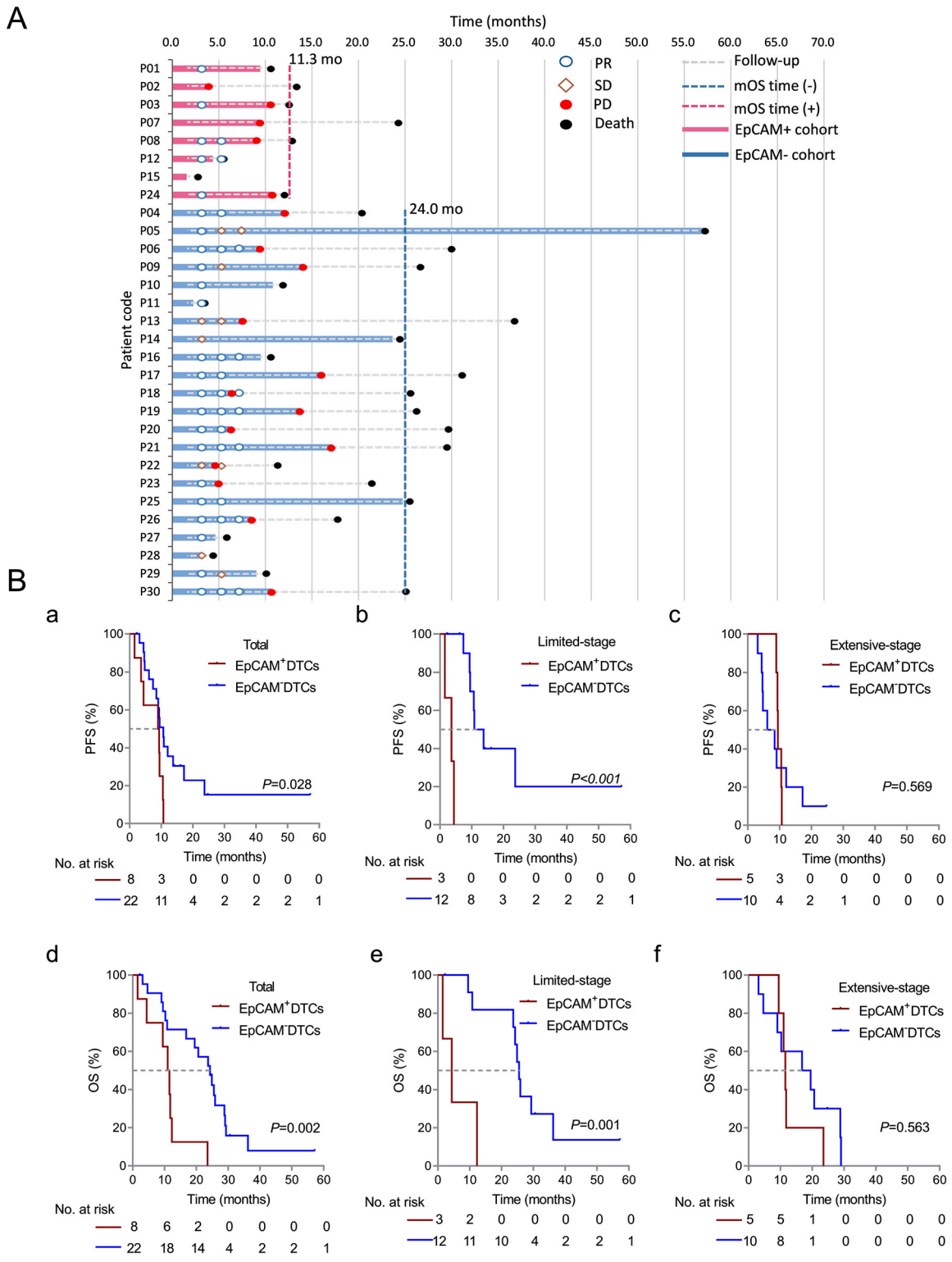

Fig. 7. Prognosis analysis of the EpCAM$^+$ DTCs and EpCAM$^-$ DTCs cohorts of patients. (A) Progressive clinical status of each subject in the EpCAM$^+$ DTCs (red) and EpCAM$^-$ DTCs (blue) cohorts is illustrated. (B) Kaplan–Meier survival analysis. (Ba) The PFS curves of overall SCLC patients with EpCAM$^+$ DTCs and EpCAM$^-$ DTCs. (Bb-c) The PFS curves of patients with EpCAM$^+$ DTCs and EpCAM$^-$ DTCs in limited-stage SCLC and extensive-stage SCLC cohorts. (Bd) The OS curves of overall SCLC patients with EpCAM$^+$ DTCs and EpCAM$^-$ DTCs. (Be-f) The OS curves of patients with EpCAM$^+$ DTCs and EpCAM$^-$ DTCs in limited-stage SCLC and extensive-stage SCLC cohorts. DTCs, disseminated tumor cells; Epcam, epithelial cell adhesion molecule; mo, months; mOS, median overall survival; PD, progressive disease; PFS, progression-free survival, Pos, positive; PR, partial response; SCLC, small cell lung cancer; SD, stable disease.

poral intra-tumor genomic heterogeneity. Importantly, post-treatment DTCs in the bone marrow exhibited a higher degree of homogenous gene mutations with pretreatment CTCs, supporting the hypothesis that the bone marrow is responsible for primary tumor cell dormancy. These findings further validate the crucial role of bone marrow sampling in SCLC research.

CTCs are typically found circulating as single cells, but they can also occasionally aggregate to form clusters known as CTM in peripheral blood. Tumor cells exhibit high heterogeneity, and different clones of cancer cells can show cooperative behavior, promoting mutual survival and metastatic ability.[28] CTC clusters, whether homotypic or heterotypic in composition, possess a greater ability to metastasize compared with single CTCs, contributing to disease progression and metastasis colonization.[29] This study disclosed that the positivity of DTM and DTEM in bone marrow was much higher than the incidence of CTM and CTEM in the blood. This finding aligns with previous research, suggesting a correlation between tumor cell clusters and the overall number of tumor cells.[30] Whether DTM and DTEM can be used to predict prognosis in SCLC patients was further investigated. Survival analysis confirmed that baseline DTM-negative patients exhibited significantly longer OS than those with DTM cluster-positive detection. Similar result was observed with respect to the association between DTEM and OS. Our data validated the notion that, in addition to the intrinsic biological functions of cancer cells, intercellular communication between cancer cells may play a crucial role in disease progression. However, further investigations are warranted to gain a better understanding of the underlying mechanisms of cancer cell-cell communication.

Aside from enumeration of total DTCs and DTECs, we performed further *in situ* phenotypic and karyotypic characterization using iFISH to depict the comprehensive atlas of DTCs and DTECs, and meanwhile confirm the presence of cells with epithelial traits in the bone marrow. Aneuploidy, characterized by chromosome gains and losses, is a hallmark of malignancy that drives lethal progression in tumor cells.[31] The aberrant alternation of chromosome 8 are one of the most common chromosomal abnormalities in lung cancer patients.[32] Studies have demonstrated that chromosome aneuploidy in carcinoma cells can influence the transcription of multiple genes,[33] resulting in a variety of phenotypes that subsequently contribute to tumor cell heterogeneity, therapeutic resistance, and tumor relapse in cancer patients.[34,35] In the present study, karyotype analysis disclosed a significant difference in the degree of chromosome aneuploidy between DTCs with or without EpCAM phenotype, which was consistent with our previous studies on other EMT-related phenotypes of CTCs.[36] These findings suggest that not only changes in cell surface makers, but also alterations in the karyotype of chromosome 8 are involved in the process of EMT. The discrepancy in karyotype composition may be attributed to the biological functions of different tumor cell types.

Growing evidence has demonstrated the significant role of cancer cells undergoing EMT in tumor initiation, chemoresistance, and disease progression in various carcinoma types, including lung cancer. Here, our result disclosed that the existence of EpCAM$^+$ CTCs in blood was not consistent with the positive detection of EpCAM$^+$ DTCs in bone marrow. This can be attributed to the bone marrow providing a suitable microenvironment that induces an EMT-like program through the interaction between tumor cell and bone marrow niches, resulting in drug resistance and enhanced survival.[37] Therefore, we aimed to evaluate the clinical significance of EpCAM$^+$ DTCs in assessing tumor response and predicting survival outcomes in SCLC patients. Our findings revealed that the baseline presence of EpCAM$^+$ DTCs was significantly correlated with a decreased DCR, suggesting that positive detection of EpCAM$^+$ DTCs may possess clinical utility in predicting SCLC patients' drug resistance to initial treatment. Survival analysis further confirmed that SCLC patients with baseline EpCAM$^+$ DTCs exhibited significantly reduced OS compared with those without EpCAM$^+$ DTCs, which was partly in line with our previous research on advanced NSCLC. Subgroup analysis revealed that EpCAM$^+$ DTCs can predict LD-SCLC but not ED-SCLC patients' poor prognosis. These results suggested that the pre-therapeutic EpCAM$^+$ DTCs may serve as prognosticators for poor treatment response and inferior clinical outcomes. In clinical trials, the EpCAM molecule can serve as a descriptive therapeutic target for cancer and EpCAM-specific antibodies have been reported to effectively eliminate cancer cells.[38,39] Although no EpCAM targeted agents are currently available in SCLC, our results provide additional perspectives with respect to the development of new EpCAM therapeutic agents for translation in the future and EpCAM$^+$ DTCs may also serve as a promising biomarker for risk stratification of SCLC patients. To further validate the clinical significance of EpCAM$^+$ DTCs, we are currently conducting expanded studies on a large cohort of SCLC patients.

Our study has several limitations that should be acknowledged. First, this study included a relatively small samples for analysis, which may limit the statistical power of the research. Second, the WES data were generated from DTCs and CTCs only, without including primary tumor tissue, which may induce the conclusions less comprehensive. Finally, the underlying mechanism of EpCAM$^+$ DTCs in treatment resistance and disease progression remains unclear and requires further investigation.

In summary, our study provides novel insights by demonstrating that the bone marrow contains a significantly higher number of DTCs and DTECs compared with their contemporaneous CTCs and CTECs. Furthermore, DTCs inherited more homologous somatic information from pretreatment CTCs compared with post-treatment CTCs. The identification of the epithelial subtype EpCAM$^+$ DTCs holds promise as a biomarker for assessing initial treatment response and predicting survival outcomes in SCLC patients. Bone marrow sampling and detection of pretreatment EpCAM$^+$ DTCs may have implications in risk stratification and personalized clinical management of SCLC patients. Additionally, the bone marrow provides an optimal alternative site for studying the heterogeneous nature of tumor cells. Further studies involving larger cohorts and serial follow-up samplings are warranted to further investigate bone marrow DTCs in SCLC.

Declaration of completing interest

The authors declare that they have no known competing financial interests or personal relationships that could have appeared to influence the work reported in this paper.

Ethics statement

All procedures performed in this study involving human participants were in accordance with the Declaration of Helsinki (as revised in 2013). The study was approved by the Ethics and Scientific Committee of Beijing Chest Hospital (approval number: KY-2018-002). Written informed consent was obtained from all subjects in this study.

Data availability

All datasets are available from the corresponding author for reasonable request.

Acknowledgments

This work was granted by Beijing Municipal Science and Technology Commission (grant number Z211100002921013), Tongzhou Lianggao Talents Project (grant number YH201920), Beijing Municipal Public Welfare Development and Reform Pilot Project for Medical Research Institutes (grant number JYY2024-14), and Beijing Municipal Public Welfare Development and Reform Pilot Project for Medical Research Institutes (grant number JYY2023-15). We thank all participants and their families for supporting this study.

Author contributions

T.Z. and X.H. designed the project; Y.W., J.N., B.L., Y.G., and M.H collected the bone marrow and blood samples; Y.W., J.N., L.Z., J.T. C.C., and X.Y. performed the experiments; Y.W. and C.C. analyzed the data. Y.W., J.N., and B.L. wrote the original draft; T.Z., X.H., and P.P. contributed to writing, review, and editing; T.Z. contributed to funding acquisition of the manuscript. The authorship order was decided based on T.Z. initiating the project. All authors read and approved the final manuscript.

Supplementary materials

Supplementary material associated with this article can be found, in the online version, at doi:10.1016/j.jncc.2024.07.003.

References

1. Yin X, Li Y, Wang H, et al. Small cell lung cancer transformation: from pathogenesis to treatment. *Semin Cancer Biol*. 2022;86:595–606. doi:10.1016/j.semcancer.2022.03.006.
2. Horn L, Mansfield AS, Szczęsna A, et al. First-line atezolizumab plus chemotherapy in extensive-stage small-cell lung cancer. *N Engl J Med*. 2018;379(23):2220–2229. doi:10.1056/NEJMoa1809064.
3. Doshita K, Kenmotsu H, Omori S, et al. Long-term survival data of patients with limited disease small cell lung cancer: a retrospective analysis. *Invest New Drugs*. 2022;40(2):411–419. doi:10.1007/s10637-021-01183-6.
4. Byers LA, Rudin CM. Small cell lung cancer: where do we go from here? *Cancer*. 2015;121(5):664–672. doi:10.1002/cncr.29098.
5. Caliman E, Fancelli S, Petroni G, et al. Challenges in the treatment of small cell lung cancer in the era of immunotherapy and molecular classification. *Lung Cancer*. 2023;175:88–100. doi:10.1016/j.lungcan.2022.11.014.
6. Ganti AKP, Loo BW, Bassetti M, et al. Small cell lung cancer, Version 2.2022, NCCN clinical practice guidelines in oncology. *J Natl Compr Canc Netw*. 2021;19(12):1441–1464. doi:10.6004/jnccn.2021.0058.
7. Huang Y, Hong W, Wei X. The molecular mechanisms and therapeutic strategies of EMT in tumor progression and metastasis. *J Hematol Oncol*. 2022;15(1):129. doi:10.1186/s13045-022-01347-8.
8. Hamilton G, Rath B. Mesenchymal-epithelial transition and circulating tumor cells in small cell lung cancer. *Adv Exp Med Biol*. 2017;994:229–245. doi:10.1007/978-3-319-55947-6_12.
9. Gires O, Pan M, Schinke H, et al. Expression and function of epithelial cell adhesion molecule EpCAM: where are we after 40 years? *Cancer Metastasis Rev*. 2020;39(3):969–987. doi:10.1007/s10555-020-09898-3.
10. Keller L, Werner S, Pantel K. Biology and clinical relevance of EpCAM. *Cell Stress*. 2019;3(6):165–180. doi:10.15698/cst2019.06.188.
11. Zhu HH, Liu YT, Feng Y, et al. Circulating tumor cells (CTCs)/circulating tumor endothelial cells (CTECs) and their subtypes in small cell lung cancer: predictors for response and prognosis. *Thorac Cancer*. 2021;12(20):2749–2757. doi:10.1111/1759-7714.14120.
12. Lin PP, Gires O, Wang DD, et al. Comprehensive in situ co-detection of aneuploid circulating endothelial and tumor cells. *Sci Rep*. 2017;7(1):9789. doi:10.1038/s41598-017-10763-7.
13. Majidpoor J, Mortezaee K. Steps in metastasis: an updated review. *Med Oncol*. 2021;38(1):3. doi:10.1007/s12032-020-01447-w.
14. Van der Toom EE, Axelrod HD, de la Rosette JJ, et al. Prostate-specific markers to identify rare prostate cancer cells in liquid biopsies. *Nat Rev Urol*. 2019;16(1):7–22. doi:10.1038/s41585-018-0119-5.
15. Liu X, Li J, Cadilha BL, et al. Epithelial-type systemic breast carcinoma cells with a restricted mesenchymal transition are a major source of metastasis. *Sci Adv*. 2019;5(6):eaav4275. doi:10.1126/sciadv.aav4275.
16. Zhang T, Zhang L, Gao Y, et al. Role of aneuploid circulating tumor cells and CD31(+) circulating tumor endothelial cells in predicting and monitoring anti-angiogenic therapy efficacy in advanced NSCLC. *Mol Oncol*. 2021;15(11):2891–2909. doi:10.1002/1878-0261.13092.
17. Sommariva M, Gagliano N. E-Cadherin in pancreatic ductal adenocarcinoma: a multifaceted actor during EMT. *Cells*. 2020;9(4):1040. doi:10.3390/cells9041040.
18. Chen Y, Li Y, Qi C, et al. Dysregulated KRAS gene-signaling axis and abnormal chromatin remodeling drive therapeutic resistance in heterogeneous-sized circulating tumor cells in gastric cancer patients. *Cancer Lett*. 2021;517:78–87. doi:10.1016/j.canlet.2021.06.002.
19. Yip RKH, Rimes JS, Capaldo BD, et al. Mammary tumour cells remodel the bone marrow vascular microenvironment to support metastasis. *Nat Commun*. 2021;12(1):6920. doi:10.1038/s41467-021-26556-6.
20. Yang CJ, Chan DY, Shah SA, et al. Long-term survival after surgery compared with concurrent chemoradiation for node-negative small cell lung cancer. *Ann Surg*. 2018;268(6):1105–1112. doi:10.1097/sla.0000000000002287.
21. Megyesfalvi Z, Barany N, Lantos A, et al. Expression patterns and prognostic relevance of subtype-specific transcription factors in surgically resected small-cell lung cancer: an international multicenter study. *J Pathol*. 2022;257(5):674–686. doi:10.1002/path.5922.
22. Zhan Q, Liu B, Situ X, et al. New insights into the correlations between circulating tumor cells and target organ metastasis. *Signal Transduct Target Ther*. 2023;8(1):465. doi:10.1038/s41392-023-01725-9.
23. Badia-Ramentol J, Linares J, Gómez-Llonin A, et al. Minimal residual disease, metastasis and immunity. *Biomolecules*. 2021;11(2):130. doi:10.3390/biom11020130.
24. Ring A, Nguyen-Sträuli BD, Wicki A, et al. Biology, vulnerabilities and clinical applications of circulating tumour cells. *Nat Rev Cancer*. 2023;23(2):95–111. doi:10.1038/s41568-022-00536-4.
25. Muscarella AM, Aguirre S, Hao X, et al. Exploiting bone niches: progression of disseminated tumor cells to metastasis. *J Clin Investig*. 2021;131(6):e143764. doi:10.1172/jci143764.
26. Sai B, Xiang J. Disseminated tumour cells in bone marrow are the source of cancer relapse after therapy. *J Cell Mol Med*. 2018;22(12):5776–5786. doi:10.1111/jcmm.13867.
27. Pantel K, Alix-Panabières C. Bone marrow as a reservoir for disseminated tumor cells: a special source for liquid biopsy in cancer patients. *Bonekey Rep*. 2014;3:584. doi:10.1038/bonekey.2014.79.
28. Li Y, Zhang X, Gong J, et al. Aneuploidy of chromosome 8 in circulating tumor cells correlates with prognosis in patients with advanced gastric cancer. *Chi J Cancer Res*. 2016;28(6):579–588.
29. Herath S, Razavi Bazaz S, Monkman J, et al. Circulating tumor cell clusters: insights into tumour dissemination and metastasis. *Expert Rev Mol Diagn*. 2020;20(11):1139–1147. doi:10.1080/14737159.2020.1846523.
30. Hou JM, Krebs MG, Lancashire L, et al. Clinical significance and molecular characteristics of circulating tumor cells and circulating tumor microemboli in patients with small-cell lung cancer. *J Clin Oncol*. 2012;30(5):525–532. doi:10.1200/jco.2010.33.3716.
31. Stopsack KH, Whittaker CA, Gerke TA, et al. Aneuploidy drives lethal progression in prostate cancer. *Proc Natl Acad Sci USA*. 2019;116(23):11390–11395. doi:10.1073/pnas.1902645116.
32. Baity M, Wang L, Correa AM, et al. Glutathione reductase (GSR) gene deletion and chromosome 8 aneuploidy in primary lung cancers detected by fluorescence in situ hybridization. *Am J Cancer Res*. 2019;9(6):1201–1211.
33. Durrbaum M, Storchova Z. Effects of aneuploidy on gene expression: implications for cancer. *Febs J*. 2016;283(5):791–802. doi:10.1111/febs.13591.
34. Sansregret L, Swanton C. The role of aneuploidy in cancer evolution. *Cold Spring Harb Perspect Med*. 2017;7(1). doi:10.1101/cshperspect.a028373.
35. Wang L, Li Y, Xu J, et al. Quantified postsurgical small cell size CTCs and EpCAM(+) circulating tumor stem cells with cytogenetic abnormalities in hepatocellular carcinoma patients determine cancer relapse. *Cancer Lett*. 2018;412:99–107. doi:10.1016/j.canlet.2017.10.004.
36. Wang Y, Liu Y, Zhang L, et al. Vimentin expression in circulating tumor cells (CTCs) associated with liver metastases predicts poor progression-free survival in patients with advanced lung cancer. *J Cancer Res Clin Oncol*. 2019;145(12):2911–2920. doi:10.1007/s00432-019-03040-9.
37. Park CS, Yoshihara H, Gao Q, et al. Stromal-induced epithelial-mesenchymal transition induces targetable drug resistance in acute lymphoblastic leukemia. *Cell Rep*. 2023;42(7):112804. doi:10.1016/j.celrep.2023.112804.
38. Hempel P, Müller P, Oruzio D, et al. Combination of high-dose chemotherapy and monoclonal antibody in breast-cancer patients: a pilot trial to monitor treatment effects on disseminated tumor cells. *Cytotherapy*. 2000;2(4):287–295. doi:10.1080/146532400539224.
39. Zhang C, Sheng W, Al-Rawe M, et al. EpCAM- and EGFR-specific antibody drug conjugates for triple-negative breast cancer treatment. *Int J Mol Sci*. 2022;23(11):6122. doi:10.3390/ijms23116122.